RSC Advances

ROYAL SOCIETY OF CHEMISTRY

www.rsc.org/advances

Electrodeposition of crystalline silicon directly from silicon tetrachloride in ionic liquid at low temperature

Junling Zhang, Shimou Chen, Haitao Zhang, Suojiang Zhang, Xue Yao and Zhaohui Shi*

Beijing Key Laboratory of Ionic Liquids Clean Process, Key Laboratory of Green Process and Engineering, State Key Laboratory of Multiphase Complex Systems, Institute of Process Engineering, Chinese Academy of Sciences, Beijing 100190, China

*Corresponding author: sjzhang@ipe.ac.cn

Abstract

Crystalline silicon (Si) is widely used in modern electronics. Si is commonly produced through a series of energy-intensive reactions (> 700 °C). It is thus urgent and significant to explore more economic and environment-benign synthetic strategies of crystalline Si at low temperature. In this contribution, we report an efficient method to prepare crystalline Si from silicon tetrachloride at low temperature of 100 °C with ionic liquid (IL) as electrolyte. Physicochemical characterizations revealed that as-deposited crystalline Si with diamond cubic crystal structure exhibited a dominant (111)-orientation. Moreover, in-depth insights into the growth mechanism of crystalline Si was shed light upon herein. Furthermore, the smart electrodepositing platform of crystalline Si from ILs would open a new avenue for low-temperature metallurgy of Si .

Keywords: Crystalline silicon; Ionic liquid; Low-temperature electrodeposition; Liquid metal electrode

1. Introduction

Si is the most important semiconductor in optoelectronic technologies because of its abundant existence, chemical stability, and excellent optical and electronic properties.[1-3] Therefore, it has been the subject of many research groups to obtain the simple and economic production process of Si. The current crystalline Si production process such as Siemens method often involves a series of energy-intensive, highly polluting carbothermal reduction reactions. In recent years, continuous increased desire for lower-cost Si-based solar photovoltaic devices has motivated the researchers to explore an alternative cheaper and greener technique for Si extraction.

Electrodeposition has been identified as a potential alternative route for the preparation of metals and semiconductors since it can be easily controlled, and is relatively clean and cheap.[4, 5] Electrodeposition of Si has been studied in various solution media such as high-temperature molten salts (fluoride molten salt, calcium chloride, *etc.*),[6, 7] organic solvents,[8, 9] and room-temperature ionic liquids (ILs).[10-13] Si can be well electrodeposited as crystalline products from molten salts at high temperatures (> 700 °C), and that often results in difficult operations and high energy consumption. Si can also be electrodeposited in organic solvents and ILs at low temperature. However, the as-prepared Si from low temperature electrodeposition is always amorphous and requiring additional high temperature thermal annealing.[14] Therefore, the incompatibility of low temperatures and a crystalline product have thus severely limited the developing of Si-electrodeposition technology. Recently, it was reported by Maldonado *et al.* that crystalline Si can be electrodeposited by using a liquid-metal working electrode at 80 – 100 °C.[15] Liquid-metal electrode can act as both the electron source for reducing dissolved species in solution and the solvent for re-crystallization. This method for Si electrodeposition overcomes the

long standing challenge and have substantial technological impact. Organic solvent propylene carbonate (PC) was employed as electrolyte in the research before.[15] There are many advantages in the use of conventional organic solvents such as being cost-effective and easy to control. However, the system suffers from high volatility which results in quick evaporation in higher temperatures. From the practical application point of view, it is still needed to develop novel electrolytes with improved physicochemical features such as low volatility and good thermal stability.

ILs behave very differently to traditional molecular liquids when they are used as solvents. ILs are usually non-volatile and have high thermal stability in most cases, which make them can be used over a wide temperature range.[16-22] Everything has two sides, ILs also have some main drawbacks such as high viscosity and cost of production. The high viscosity often causes some difficulties in their handling. Bis(trifluoromethylsulfonyl)imide anion ($TFSI^-$) is one of the most popular anions in ILs chemistry which is widely used because it is known to produce ILs with a low melting point and low viscosity (**Table S1**, ESI†). By comparing cyclic voltammetry (CV) performance of $SiCl_4$ in three different ILs (**Fig. S1**, ESI†), Tri-1-butylmethylammonium bis((trifluoromethyl)sulfonyl)amide ($[N_{4441}][TFSI]$) IL was adoped in this study.Viscosity - temperature dependency of $[N_{4441}][TFSI]$ was shown in **Table S2**, ESI†. The viscosity of $[N_{4441}][TFSI]$ decreases to 30.6 mPa·s with the temperature increasing to 80 ºC. Many pioneering works have been shown that ILs are suited well for the electrodeposition of Si. Endres *et al.* obtained semiconducting Si films on highly oriented pyrolytic graphite (HOPG) and Au (111) solid electrodes in ILs such as 1-butyl-1-methylpyrrolidinium bis(trifluorom ethylsulfonyl)amide ($[Py_{14}]$ TFSI).[10, 13, 23] By using EQCM measurements, Komadina *et al.* also studied the electrodeposition of Si from trimethyl-n-hexyl ammonium bis-(trifluoromethylsulfonyl)

amide([TMHA][TFSI]) ionic liquid, and they found that the deposition of Si occurs *via* a four-electron reduction step.[24] It was also reported by Katayama and co-workers that a thin Si layer can be electrodeposited in 1-ethyl-3-methylimidazolium hexafluorosilicate([EMIM][SiF_6]). However, upon exposure to air the deposits reacted completely to SiO_2, which makes it difficult to make sure whether the deposit was semiconducting or not.[25] To the best of our knowledge, there is still no report on crystalline Si directly electrodeposited from ILs at low temperature. Herein, we reported data demonstrating the use of hydrophobic [N_{4441}][TFSI] IL and Ga liquid metal electrode as a platform for direct electrodeposition of crystalline Si from the dissolved $SiCl_4$ precursor under benign conditions.

2. Experimental

Materials and chemicals Lithium bis(trifluoromethylsulfonyl)imide was purchased from SCM Industrial Chemical Co. Ltd. Butyltrimethylammonium chloride was purchased from Anhui benma apex technology Co. Ltd. Silicon tetrachloride ($SiCl_4$, 99.998%) was purchased from Alfa Aesar. Gallium (Ga, 99.99%) was purchased from Aladdin. All the chemicals used in this work were purchased commercially with analytic grade and used as received.

Preparation and characterization of [N_{4441}][TFSI] [N_{4441}][TFSI] was prepared by mixing the aqueous solutionsofbutyltrimethylammonium chloride (1 mol) and lithium bis(trifluoromethylsulfonyl)imide (1.05 mol) at room temperature (RT) under magnetic stirring for 3 h. The colorless IL phase at the lower layers was separated with a separatory funnel. The separated IL was washed with ultrapure water for several times to remove the reactants. The [N_{4441}][TFSI] was dried under vacuum for 24 h at 100 °C to remove the volatiles and reduce water contents to under 10 ppm (by Karl-Fischer titration). The processed [N_{4441}][TFSI] IL was stored in a sealed bottle in an argon-filled glove box (MIKROUNA Universal, O_2 below 1 ppm,

H_2O below 1 ppm). The viscosity of $[N_{4441}][TFSI]$ was measured with an automated microviscometer (Anton Paar AMVn, Anton Paar Co., Austria) with relative expanded uncertainty Ur (η) = 0.005 (0.95 level of confidence). Calibration was performed using viscosity standard oils (No. H117, Anton Paar Co.). The temperature of the sample was maintained to ±0.1 K *via* a built-in precise Peltierthermostat.

Electrodeposition of Si A single compartment electrochemical cell with three electrodes (**Fig. S2**, ESI†) was used to probe the electrochemical window and electrodepositing behavior of Si. A quartz beaker of 50 ml was used as the electrochemical cell. 400 μL Ga (*l*) pool was employed as the working electrode (*ca.* 0.785 cm^2 active area). Pt wire (99.99%, 0.5 mm in diameter) coated by a heat shrink tube was dipped into the liquid gallium for electrical connection. A Pt plate (99.99%, 10 mm × 20 mm × 0.1 mm) was used as counter electrode. Ag electrode (silver wire with 99.99% in purity and 0.5mm in diameter) was used as quasi-reference electrode in CV studies. The counter electrode (Pt plate) was mechanically polished with 0.05 μm alumina to a mirror finish and ultrasonically washed in ultrapure water for 3 min, rinsed out with ethanol and finally dried with cold N_2 flow. Electrochemical measurements were performed using a CHI660 Electrochemical workstation (Shanghai Chenhua, China). All the electrochemical experiments were carried out in the argon-atmosphere glove box.

Material Characterizations X-ray photoelectron spectra (XPS) were recorded with an X-ray photoelectron spectrometer (Thermo Fisher Scientific, Escalab 250Xi), utilizing a monochromatic Al-Kα X-ray source, hybrid optics and a multi-channel plate and delay line detector coupled to a hemispherical analyzer. All the spectra were recorded using an aperture slot of 300 μm × 700 μm, and high resolution spectra were collected with pass energy of 20 eV. The pressure in the analysis chamber was typically 2×10^{-9} Torr during data acquisition. All binding

energies were referenced to C 1s (284.5 eV) binding energy for data analysis. Raman spectra were obtained on a LabRAM HR800 (514 nm wavelength, 4 mW power, Horiba JobinYVon, France). Ramanspectroscopy was simultaneously performed in the ambient atmosphere at RT. Bulk powder X-ray diffractograms (XRD) were collected with Empyrean, PANalytical B. V. equipped with a Cu Kα source (λ = 1.5406 Å). Scanning electron micrographs (SEM) were taken at 5 kV with a Hitachi SU8020 SEM equipped with an SE/BSE detector. Energy dispersive spectra were taken at 20 kV with an Auger electron spectroscopy detector (AES, JAMP-9500F, accelerating voltage: 10 kV, JEOL Ltd.). High-resolution transmission electron microscopy (HRTEM) and selected area electron diffraction (SAED) were performed with a JEM-2100F UHRTEM equipped with a LaB_6 source operated at 200 kV.

3. Results and Discussion

3.1. Electrodeposition of Si

In order to determine the cathodic limit of IL stability and to study Si reduction in $SiCl_4$/ $[N_{4441}][TFSI]$, CV was performed. **Fig. 1** shows the cyclic voltammetric responses for $SiCl_4$ reduction on Ga liquid metal electrodes at the first negative scan at 100 °C. For the pristine IL, irreversible reduction of the organic cation can be observed at the potential -2.7 V (*vs.* Ag QRE). A rather weak voltammetric wave (C1) was also observed at approximately -1.39 V which probably was caused by cleavage of the S–N bond in the anion.[26] The voltammetry performed in $SiCl_4$ containing ionic liquid (0-500 mM) displayed two main reduction peaks (C2 and C3). The observed cathodic wave (C2) at -1.22 V can be attributed to the underpotential deposition Si on Ga electrode. The peak at round -1.86 V followed by a more negative wave indicated the bulk deposition. For 250 mM $SiCl_4$ containing IL solution, the voltammetric response showed a clear diffusion-limited wave at -2.3 V (*vs.* Ag QRE), which could be separated from the onset of

cathodic solvent decomposition. The present voltammetry data differs from the results reported for the electroreduction of $SiCl_4$ in propylene carbonate.[15] In the latter process, diffusion-controlled peak was observed only at lower $SiCl_4$ concentration and lower temperature, such as 100 mM at RT. This indicates that, compared with propylene carbonate organic system, IL $[N_{4441}][TFSI]$ has better electrochemical stability.

Potentiostatic electrolysiswas used to electrodeposit Si onto liquid metal electrode at -2.3 V (*vs.* Ag QRE). **Fig. 2** shows current-time curves of the electrodeposition process with different electrodepositing time. Formation and growth of the Si crystals in deposition process could be generally divided into three sections: rapid nucleation and growth in the first ten minutes (Part I), crystal growth in the next two hours (Part II) and a period of slow-growing (Part III). In fact, Si electrodeposition differs from metal deposition, the deposited layer is semiconductor which has lower conductivity than metal electrode. The reduced conductivity of working electrode surface would complicate the electron transfer through the deposit and prevent a continuous deposition reaction.[27] This could explain that the rapidly decrease of current with time, as observed in **Fig. 2**. Morphology of the deposited Si was characterized by SEM. Interestingly, two sides (see **Fig. 3a**) of the deposited Si layer have completely distinct morphological properties. As shown in **Fig. 3b** and **Fig. 3c**, side A (face to electrolyte) has a relatively smooth morphology and side B (face to liquid metal electrode) is a polycrystalline layers composed by gathering of nano-sized crystals. TEM and SAED were performed in order to determine the structure difference of the two sides. TEM image and SAED pattern of the side A were shown in **Fig. 3d** and the inset of **Fig. 3d**, respectively. Diffraction pattern in **Fig. 3d** shows that side A, which can be quickly formed at the beginning of the reaction, is amorphous in structure. **Fig. 3e** shows the TEM image of the crystal grain. Lattice fringes could not be discernable for the large size of the grain. SAED was also used

to determine the structure of particles on side B. The observed diffraction pattern showed in the inset of **Fig. 3e** is consistent with a diamond cubic lattice as expected for a single crystal of Si. TEM and SAED patterns of Si particles and films that electrodeposited for 2 h by this method were also checked (**Fig. S3**, ESI†). The diffraction characteristics of the deposited samples are similar to that showed in **Fig. 3**.

The crystal growth on side B was investigated by electrodepositing for different lengths of time. **Fig. 4** shows a series of SEM images of Si deposits on side B. High magnification image shows that Si deposit is spherical silicon particles range from 100 to 500 nm on the amorphous film at the first 10 min (**Fig. 4a**). Cone-shape particles with dominant size of 0.5 – 0.8 μm were formed in the next 1 h (**Fig. 4b**). Every particle showed sharp facets after the electrodeposition for 4 h (**Fig. 4c**), and gradually grown to polyhedrons, the size is about 2 – 3 μm in 8 h (**Fig. 4d**). The increasing of size and sharpness of the crystals were attributed to the using of liquid-metal electrodes which can act as both an electron source for reducing dissolved species in solution and a solvent for re-crystallization, and this process was named electrochemical liquid-liquid-solid (ec-LLS) process. [15]

3.2. Effect of working electrode disturbance on the morphology of Si deposits

$SiCl_4$ can be electro-reduced to Si at the surface of solid metal electrode and producing amorphous film has been proved previously.[13, 14] Crystal Si can be electrodeposited from liquid metal electrode by an ec-LLS process also was reported.[15] However, deposited Si with two different side was observed in this study and the crystal layer seems grow on the amorphous film. In order to study the catalyst or induced effects of the amorphous film on re-crystallization of Si in the liquid metal,[28, 29] a magnetic stick was adopted into the liquid metal electrode pool in the electrodeposition process which could rupture the initially formed amorphous film on the surface

of the liquid metal electrode. SEM images of the as-electrodeposited Si layer are shown in **Fig. 5**. Similar to the deposits on static working electrode, uniformly sized crystal particles were consistently observed on an amorphous film with total widths of 1 – 2 μm (**Fig. 5a, b**). However, crystal particles produced on stirred working electrode surface grew along a certain line instead of closely packed, showed mesh-like distributing on amorphous film (**Fig. 5c, d**).

The nucleation and growth of Si requires a large amount of energy. Si likely to crystallization and growth in the solid film on the electrode surface rather than inner of the liquid metal electrode because the amorphous Si has nuclei effect. Furthermore, when energy of amorphous surface distributed unevenly, Si in liquid electrode tends to crystallize along the higher energy lines. Amorphous film deposited initially on the liquid metal electrode was cracked and wrinkled by magnetic stirring. In the effect of external electric field, energy distribution on the wrinkled electrodeposited films became more uneven. Crystal preferentially grew on high energy points of the wrinkled films, consequently the Si crystals with continuous net structure were formed. SEM and corresponding element mapping images of Si deposits prepared on the liquid metal electrode without (**Fig. S4**, ESI†) and with magnetic stirring (**Fig. S5**,ESI†) are all showed that crystal Si particles are grown on thin film of Si. Furthermore, both amorphous and crystal phases can be observed in the Raman spectrum of the as-prepared Si (**Fig. S6**, ESI†). From the above discussion, we can reach that amorphous Si film has inductive effect on Si re-crystallization in the ec-LLS process, then the polyhedron crystal particles with sharp facets formed. The lowest temperature demonstrated here (100 °C) significantly favors for better electrodeposition of crystalline Si over both of the previous reports.[30, 31]

3.3. Crystal structures and composition analysis of Si deposits

Crystallographic orientation of the deposited Si in the ionic liquid was determined using

XRD. As shown in **Fig. 6a**, the as-deposited sample at 100 °C yielded sharp diffraction peaks at 2θ = 28.4 °, 47.2 ° and 56.0 ° which are perfectly matched with the diffraction from the (111), (220) and (311) orientations of crystalline Si with the diamond cubic crystal structure, respectively. The result shows that the deposited Si were polycrystalline without detectable impurity phase and having the preferred crystallographic growth orientation of (111). This crystallization is also confirmed by Raman spectrum of the freshly deposited Si sample. **Fig. 6b** displays the Raman spectra obtained at 514 nm. High power laser can facilitate crystallization of amorphous Si and affect the judgment of material structure. Spectra obtained by focusing the laser spot with different power from 0.4 to 4.0 mW on the as-deposited Si are compared in **Fig. 6b**. There is an obvious Raman peak in every curve inspired by different laser powers, which represent the crystalline Si was formed at the electrodepositing process. Raman peaks range from 501 to 508 cm^{-1} is slightly down-shifted than that of bulk Si at 520 cm^{-1}. Furthermore, the peaks are also red-shifted and dissymmetrical broadened with the increasing of laser power which demonstrated phonon confinement of the crystal Si that may arise from micro-size of crystalline.[32]

Energy-dispersive spectrometry (EDS) elemental mapping image (**Fig. 7b**) and EDS spectrum (**Fig. 7c**) revealed that both the micro-crystal grain and amorphous film are mainly the formed Si. The EDS spectrum of the Si deposit also suggests that the deposited Si is quite pure and the amounts of other elements, such as, C and Ga, are related to the process of deposits separation. The successful reduction of silicon tetrachloride to elemental silicon (Si^0) was confirmed by X-ray photoelectron spectroscopy (XPS) of the Si deposit (**Fig. 7b**). The presence of SiO_2 in the deposits should be due to the surface oxidization of the Si by air during the transfer of the prepared sample.

3.4. Growth mechanism of electrodeposited crystal Si

The mechanism for the direct electrodeposition of crystalline Si on liquid electrode from ILs is complicate, and still unknown so far. We just can propose some possible process by referring to the experimental results and the literatures. As illustrated in **Fig. 8**, the formation of crystalline Si is divided into 3 stages. At the first stage, oxidized precursor ($SiCl_4$) was electro-reduced to the fully reduced state (Si) at the surface of liquid metal electrode and producing purely amorphous Si film. As the deposition going, the thickness of the amorphous layer quickly increases, making the surface of liquid electrode more resistant and deposite current dropped rapidly (see **Fig. 2**). The formation of amorphous Si layer by electrodepositing from $SiCl_4$/IL solution has been investigated at solid electrodes previously.[10, 13, 14, 23, 33, 34] The difference is that, when a liquid metal electrode Ga (*l*) is used, the initially produced Si could be diffused into the liquid Ga phase. According to the published metallurgical data,[35] the solubility of Si in Ga between RT and 100 °C ranges from 10^{-8} to 10^{-6} at.%. At stage II, Si at the interface of amorphous layer and liquid electrode dissolved into Ga (*l*) and reached saturation and supersaturating conditions with continually reduction of $SiCl_4$ at the electrode surface. When a critical supersaturating conditions reached, phase separation of Si(s) from Ga (*l*) followed by nucleation would occur. Solubility of Si in Ga (*l*) is low, amorphous Si-induced crystal separating is more inclined to occur on the interface of amorphous Si and Ga (*l*). At stage III, as continuous crystallization and oriented attachment going on the inner surface, the polyhedron crystal particles with sharp facets formed. In other words, initially formed amorphous Si layer on the electrode surface might induce the crystallization of Si. Finally, perfect large single crystals were obtained successfully by dissolution and re-precipitation of Si in the stage III. To check the universality of this method for preparation of cystalline Si, N-Propyl-N-methylpiperidinium bis((trifluoromethyl)sulfonyl)imide

([PP_{13}] [TFSI]) was also used as electrolyte for the deposition of Si. Crystaline Si (**Fig. S7**,ESI†) also can be successfully prepared in [PP_{13}] [TFSI] at 100 °C.

4. Conclusions

In conclusion, we successfully prepared crystalline Si *via* an appealing low-temperature electrodeposition strategy. Herein, the IL of [N_{4441}][TFSI] and Ga (*l*) were utilized as electrolyte and liquid-metal electrode, respectively, which are the key factors to fabricate crystalline Si at the mild operating conditions (atmospheric pressure and 100 °C). The [N_{4441}][TFSI] rendered it possible to electrodeposit at low pressure for a long time. Liquid Ga acted as a separate phase for re-crystallization of Si at low temperature. Growth mechanism of crystalline Si was tentatively proposed including first formation of solution of Si in liquid-metal Ga, and following nucleation and growth of crystal Si on the reduced amorphous Si film. We also envision that the synthetic approach can be easily generalized to fabricate high-purity Si directly from $SiCl_4$ or $SiHCl_3$ just with a single step. More significantly, it offers an appealing avenue for scalable, economic and green fabricating process for low-temperature Si metallurgy.

Acknowledgements

This work was financially supported by the National Basic Research Program of China (No. 2015CB251401), the National Nature Science Foundations of China (No. 51274181, 21276257), Beijing Municipal Natural Science Foundation (No. 2132054).

†Electronic Supplementary Information (ESI) available: viscosity of ILs, CV in different ILs, schematic illustration of the electrolytic cell, TEM and SAED of the deposits, EDS mapping images, Raman spectrum of Si deposits and SEM images of the deposits prepared from [PP_{13}][TFSI] IL in this study.

References

[1] Y. Cui and C. M. Lieber, *Science*, 2001, **291**, 851.

[2] K. Sun, S. H. Shen, Y. Q. Liang, P. E. Burrows, S. S. Mao and D. L. Wang, *Chem. Rev.*, 2014, **114**, 8662.

[3] Y. Xiao, X. Li, H. D. Um, X. Gao, Z. Guo and J. H. Lee, *Electrochim. Acta*, 2012, **74**, 93.

[4] W. Simka, D. Puszczyk and G. Nawrat, *Electrochim. Acta*, 2009, **54**, 5307.

[5] F. Endres, *Chem. Ing. Tech.*, 2011, **83**, 1485.

[6] E. J. Frazer and B. J. Welch, *Electrochim. Acta*, 1977, **22**, 1179.

[7] T. Nohira, K. Yasuda and Y. Ito, *Nat. Mater.*, 2003, **2**, 397.

[8] Y. Nishimura and Y. Fukunaka, *Electrochim. Acta*, 2007, **53**, 111.

[9] T. Munisamy and A. J. Bard, *Electrochim. Acta*, 2010, **55**, 3797.

[10] S. Z. El Abedin, N. Borissenko and F. Endres, *Electrochem. Commun.*, 2004, **6**, 510.

[11] R. Al-Salman, S. Z. Abedin and F. Endres, *Phys. Chem. Chem. Phys.*, 2008, **10**, 4650.

[12] Y. Nishimura, T. Nohira, T. Morioka and R. Hagiwara, *Electrochem.*, 2009, **77**, 683.

[13] G. Pulletikurthi, A. Lahiri, T. Carstens, N. Borisenko, S. Z. El Abedin and F. Endres, *J Solid State Electrochem.*, 2013, **17**, 2823.

[14] M. Bechelany, J. Elias, P. Brodard, J. Michler and L. Philippe, *Thin Solid Films*, 2012, **520**, 1895.

[15] J. S. Gu, E. Fahrenkrug and S. Maldonado, *J. Am. Chem. Soc.*, 2013, **135**, 1684.

[16] Z. N. Wang, Y. J. Cai, T. Dong, S. M. Chen and X. M. Lu, *Ionics*, 2013, **19**, 887.

[17] J. P. M. Veder, M. D. Horne, T. Ruther, A. M. Bond and T. Rodopoulos, *Electrochem. Commun.*, 2012, **18**, 85.

[18] L. Liu, X. M. Lu, Y. J. Cai, Y. Zheng and S. J. Zhang, *Aust. J. Chem.*, 2012, **65**, 1523.

[19] Q. Sun, Z. Q. Hu, Y. J. Cai, T. Dong and X. M. Lu, *Chin. J. Process Eng.*, 2012, **12**, 340.

[20] Y. Zheng, S. J. Zhang, X. M. Lu, Q. Wang, Y. Zuo and L. Liu, *Chin. J. Chem. Eng.*, 2012, **20**, 130.

[21] G. K. Yue, S. J. Zhang, Y. L. Zhu, X. M. Lu, S. C. Li and Z. X. Li, *AIChE J.*, 2009, **55**, 783.

[22] Q. Q. Zhang, Q. Wang, S. J. Zhang and X. M. Lu, *J. Solid State Electrochem.*, 2014, **18**, 257.

[23] N. Borisenko, S. Z. El Abedin and F. Endres, *J. Phys. Chem. B*, 2006, **110**, 6250.

[24] J. Komadina, T. Akiyoshi, Y. Ishibashi, Y. Fukunaka and T. Homma, *Electrochim. Acta*, 2013, **100**, 236.

[25] Y. Katayama, M. Yokomizo, T. Miura and T. Kishi, *Electrochem.*, 2001, **69**, 834.

[26] P. C. Howlett, E. I. Izgorodina, M. Forsyth and D. R. MacFarlane, *Z. Phys. Chem.*, 2006, **220**, 1483.

[27] W. J. Weydanz, M. W. Mehrens and R. A. Huggins, *J. Power Sources*, 1999, **81**, 237.

[28] K. Kang, H. S. Lee, D. W. Han, G. S. Kim, D. Lee, G. Lee, Y. M. Kang and M. H. Jo, *Appl. Phys. Lett.*, 2010, **96**, 053110.

[29] S. K. Cho, F. R. F. Fan and A.J. Bard, *Angew. Chem. Int. Ed.*, 2012, **51**, 12740.

[30] G. M. Rao, D. Elwell and R. S. Feigelson, *J. Electrochem. Soc.*, 1980, **127**, 1940.

[31] W. Xiao, X. Wang, H. Y. Yin, H. Zhu, X. H. Mao and D. H. Wang, *RSC Adv.*, 2012, **2**, 7588.

[32] S. Piscanec, A. C. Ferrari, M. Cantoro, S. Hofmann, J. A. Zapien, Y. Lifshitz, S. T. Lee and J. Robertson, *Mat. Sci. Eng. C*, 2003, **23**, 931.

[33] Z. G. Li, H. L. Zhang, J. M. Du, B. X. Han and J. Q. Wang, *Colloid Surface A*, 2006, **286**, 117.

[34] F. Bebensee, N. Borissenko, M. Frerichs, O. Hofft, W. Maus-Friedrichs, S. Z. El Abedin and F. Endres, *Z. Phys. Chem.*, 2008, **222**, 671.

[35] R. W. Olesinski, N. Kanani and G. J. Abbaschian, *Bulletin of Alloy Phase Diagrams*, 1985, **6**, 362.

Figures and Captions

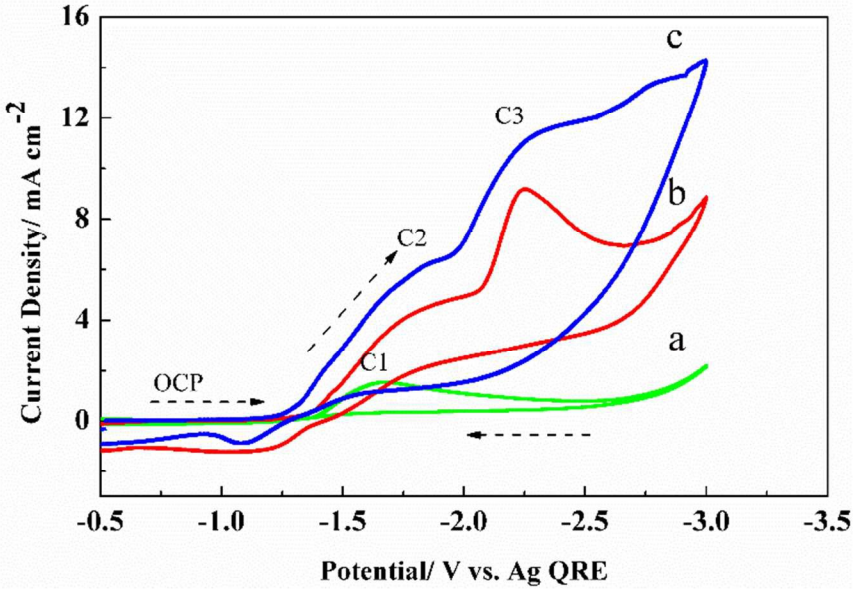

Fig. 1 Cyclic voltammetric response of the Ga (*l*) electrode in the IL of tri-1-butylmethylammonium bis((trifluoromethyl)sulfonyl)amide ($[N_{4441}][TFSI]$) with various concentrations of $SiCl_4$ (a, 0 mM; b, 250 mM; c, 500 mM) in solution at 100 °C under Ar. Scan rate is 0.05 V s^{-1}

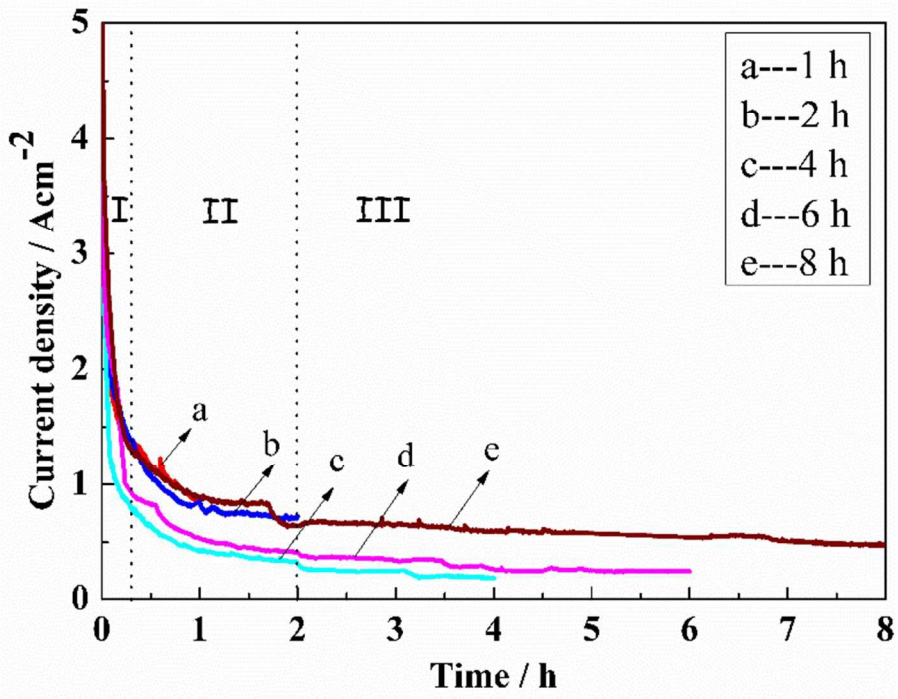

Fig. 2 Current-time curves of the potentiostatic electrodeposition process at -2.3 V (*vs.* Ag QRE) for different time (1 h, 2 h, 4 h, 6 h and 8 h) at 100 °C. The concentration of $SiCl_4$ is 250 mM

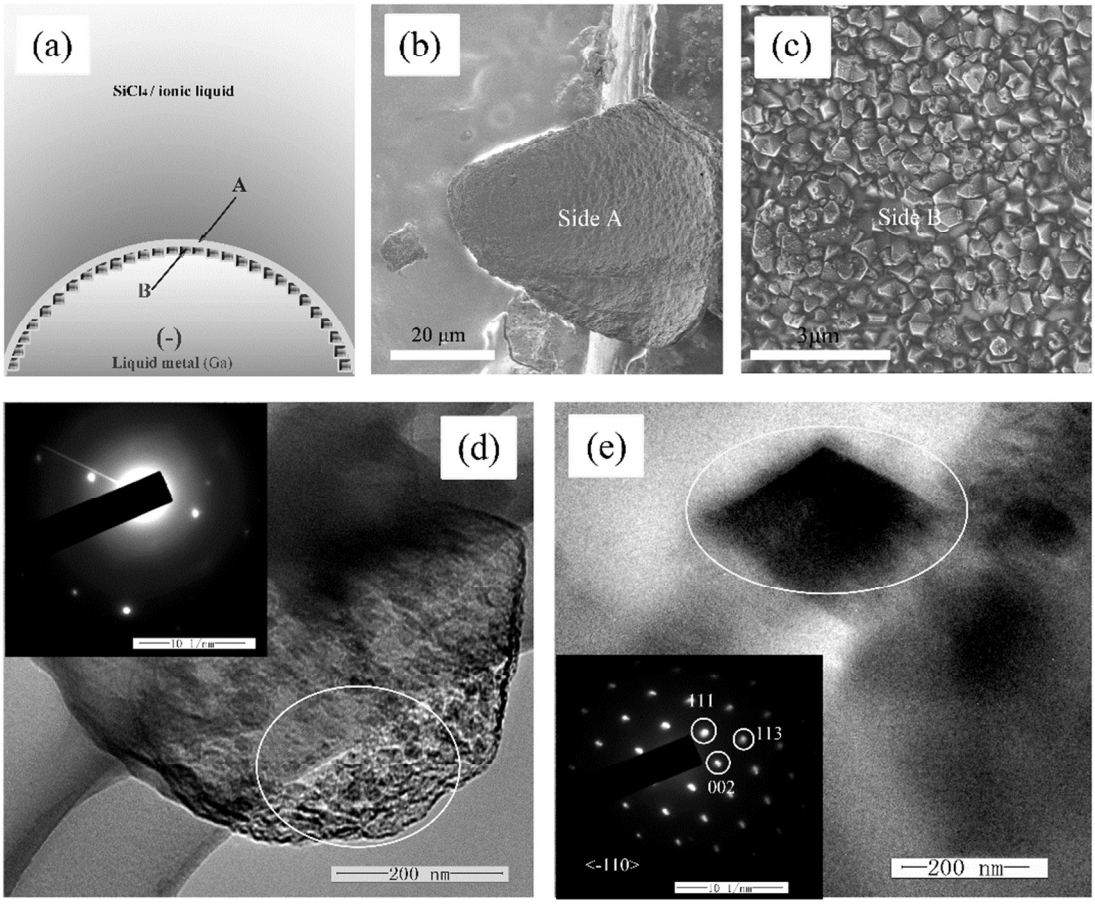

Fig. 3 (a) Illustration of the electrodeposited silicon, (b) SEM micrograph of side A, (c) SEM image of the side b, (d) TEM and SAED (the inset) of side A and (e) TEM and SAED (the inset) of the side B. The deposits were prepared at -2.3 V (vs. Ag QRE) for 4 h and maintained at 100 °C. The concentration of $SiCl_4$ is 250 mM

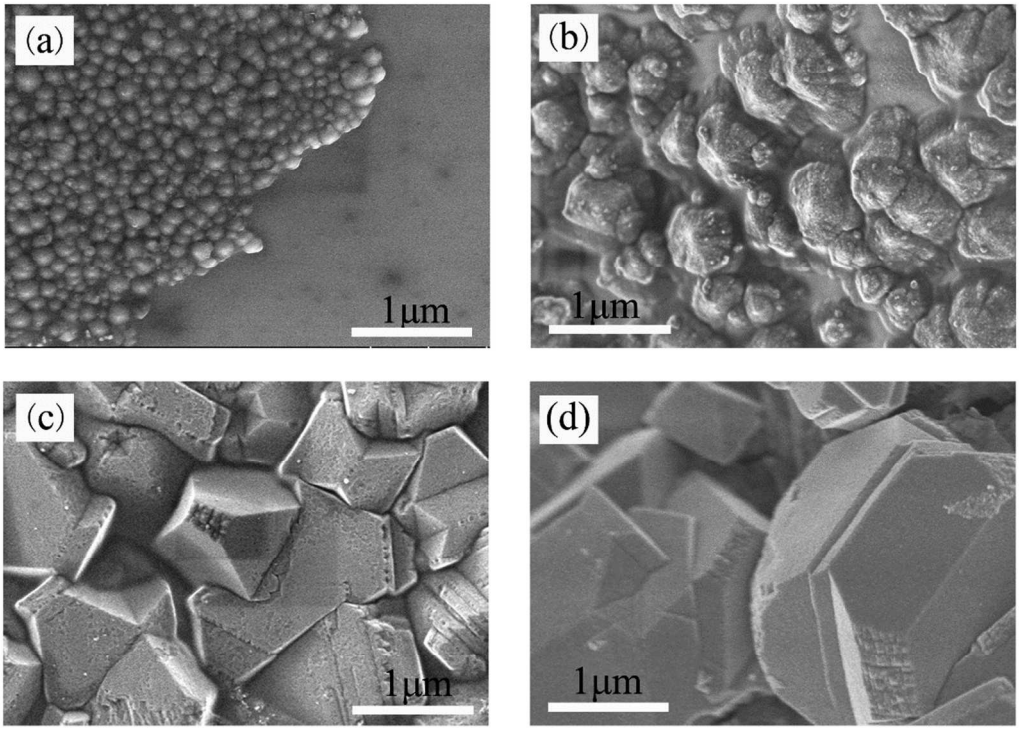

Fig. 4 SEM images of the deposits prepared at -2.3 V (*vs.* Ag QRE) with different depositing time (a, 10 min; b, 1 h; c, 4 h; d, 8 h) at 100 °C. The concentration of $SiCl_4$ is 250 mM

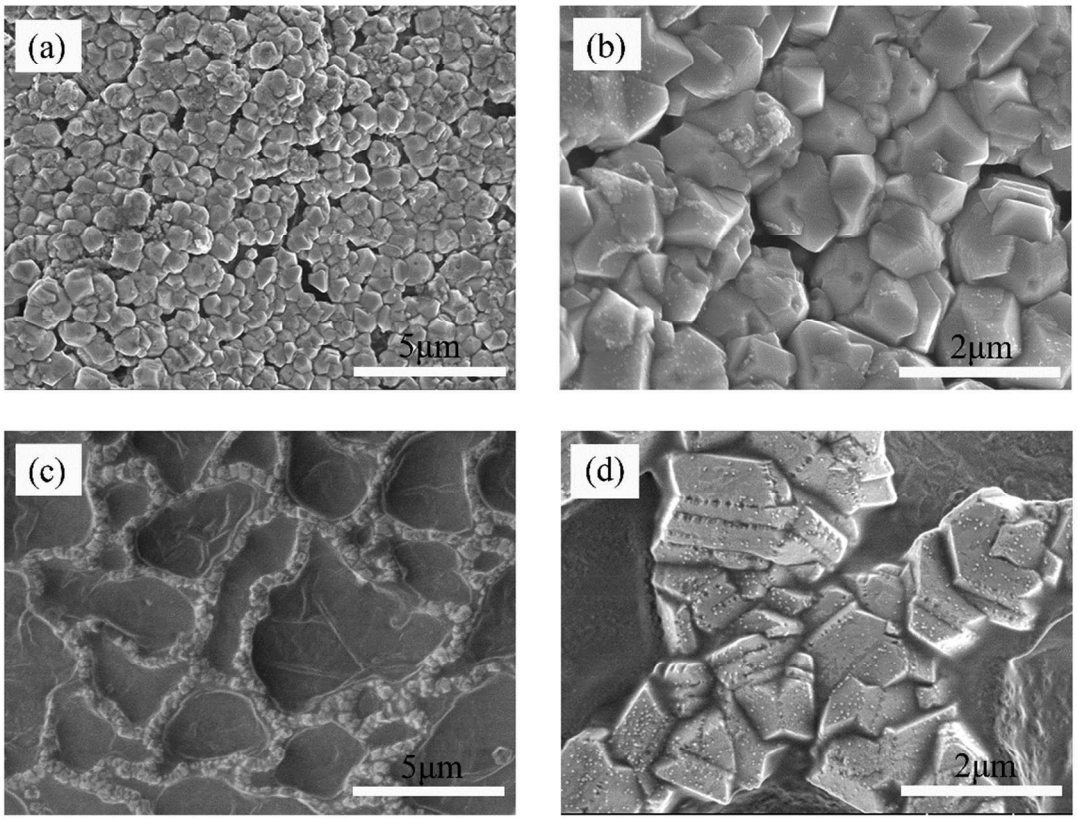

Fig. 5 SEM images of the deposits prepared on the liquid metal electrode (a, b) without and (c, d) with magnetic stirring (200 rpm). Crystalline Si grown at -2.3 V (*vs.* Ag QRE) in the IL of $[N_{4441}][TFSI]$ containing of 250 mM $SiCl_4$ at 100 °C for 8h

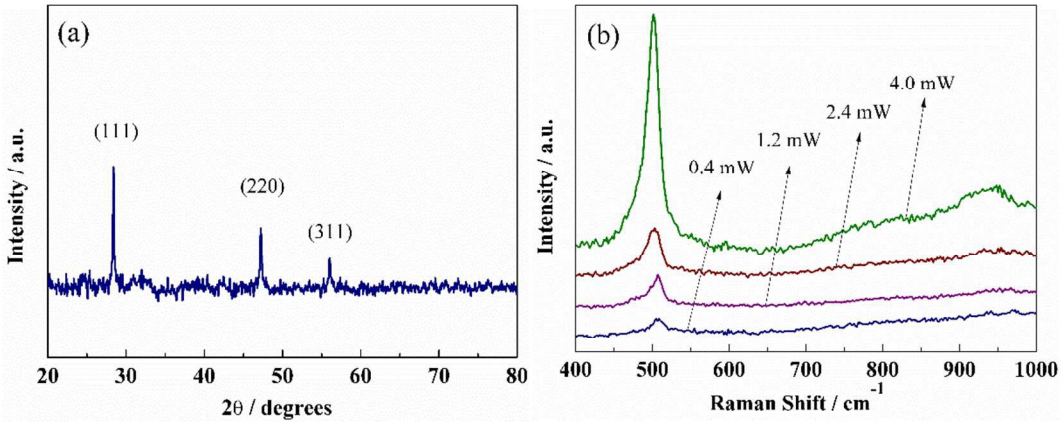

Fig. 6 (a) XRD pattern and (b) Raman spectra of the silicon deposit grown at -2.3 V (*vs.* Ag QRE) at 100 °C in the IL of $[N_{4441}][TFSI]$ containing of 250 mM $SiCl_4$

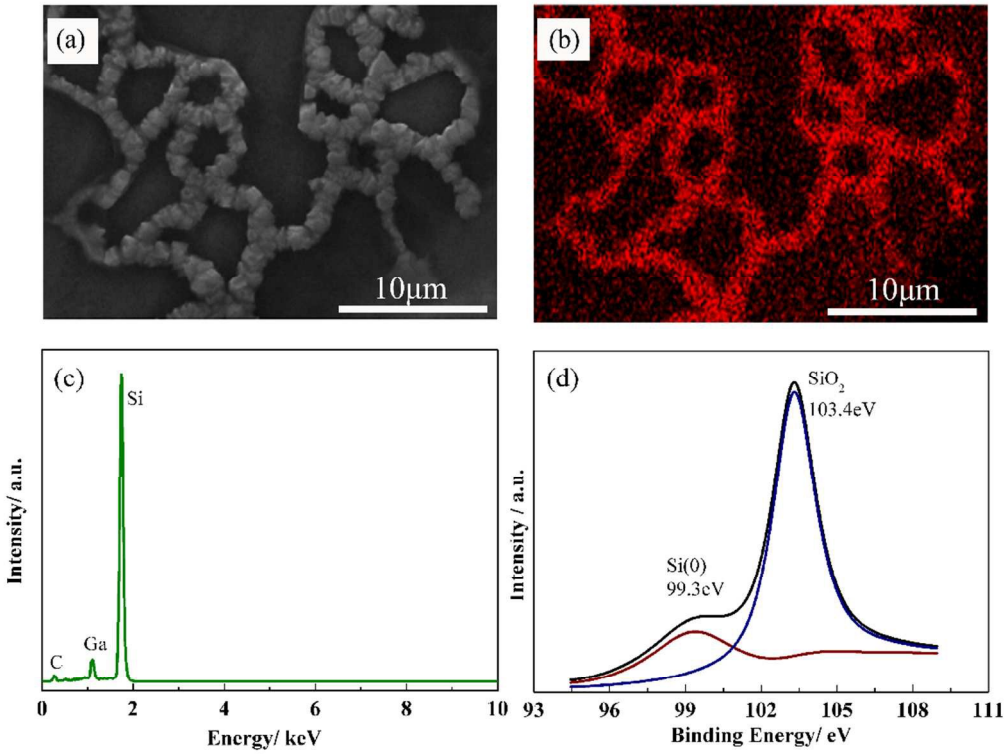

Fig. 7 (a) SEM and (b) corresponding EDS elemental mapping images, (c) EDS and (d) XPS spectra of the Si deposited at -2.3 V (*vs.* Ag QRE)

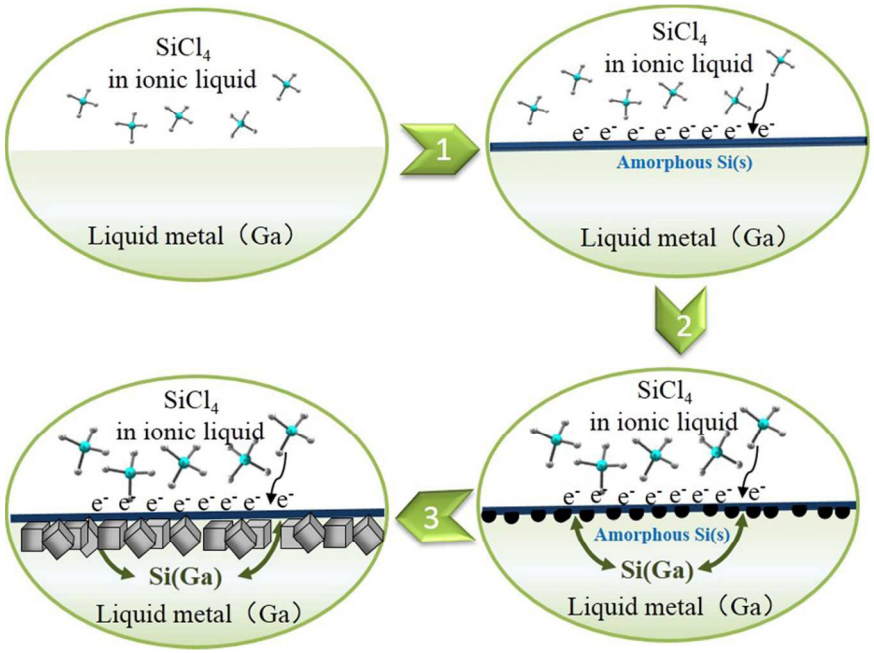

Fig. 8 Schematic illustration of crystalline Si formed on the liquid metal electrode from ILs by electrodeposition

Graphical Abstract

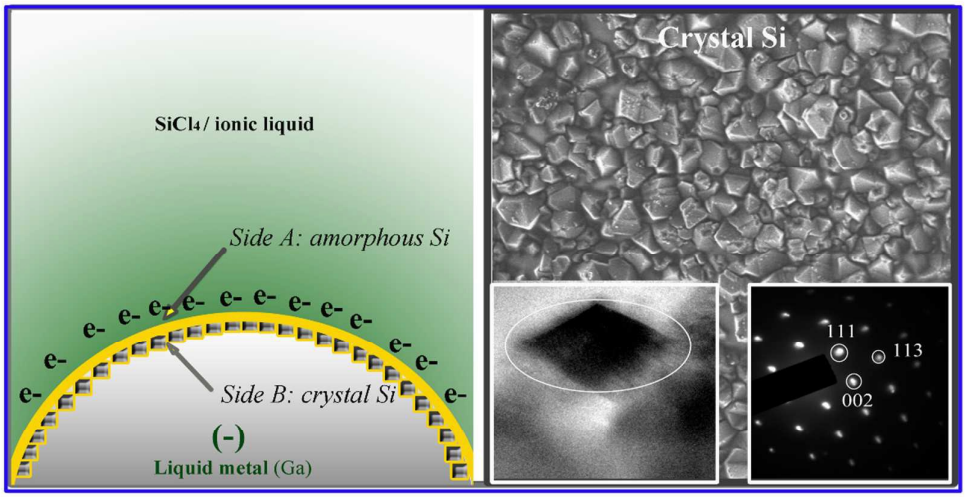

Crystalline silicon was fabricated directly from silicon tetrachloride in ionic liquid at low temperature of 100 ℃. SEM, TEM and SEAD revealed that as-deposited crystalline Si with diamond cubic crystal structure.